



**HAL**  
open science

## Dual Cross-Linked Stimuli-Responsive Alginate-Based Hydrogels

Michel Habib, Steve Berthelon, Laurent Leclercq, Audrey Tourrette, Tahmer Sharkawi, Sebastien Blanquer

► **To cite this version:**

Michel Habib, Steve Berthelon, Laurent Leclercq, Audrey Tourrette, Tahmer Sharkawi, et al.. Dual Cross-Linked Stimuli-Responsive Alginate-Based Hydrogels. *Biomacromolecules*, 2024, 25 (3), pp.1660-1670. 10.1021/acs.biomac.3c01201 . hal-04533584

**HAL Id: hal-04533584**

<https://hal.umontpellier.fr/hal-04533584v1>

Submitted on 17 Oct 2024

**HAL** is a multi-disciplinary open access archive for the deposit and dissemination of scientific research documents, whether they are published or not. The documents may come from teaching and research institutions in France or abroad, or from public or private research centers.

L'archive ouverte pluridisciplinaire **HAL**, est destinée au dépôt et à la diffusion de documents scientifiques de niveau recherche, publiés ou non, émanant des établissements d'enseignement et de recherche français ou étrangers, des laboratoires publics ou privés.

# Dual Cross-linking for Stimuli Responsive Alginate Based Hydrogels

Michel Habib<sup>1,2</sup>, Steve Bertholon<sup>1</sup>, Laurent Leclercq<sup>3</sup>, Audrey Tourrette<sup>2</sup>, Tahmer Sharkawi<sup>1\*</sup>,  
Sebastien Blanquer<sup>1\*</sup>

<sup>1</sup>ICGM, Univ Montpellier, CNRS, ENSCM, Montpellier, France

<sup>2</sup>CIRIMAT, Université Toulouse 3 Paul Sabatier, Toulouse INP, CNRS, Université de Toulouse, Toulouse,  
France

<sup>3</sup>IBMM, Univ Montpellier, CNRS, Montpellier, France

KEYWORDS: Hydrogels, polysaccharide, Sodium alginate, dual crosslinking, stimuli-responsive.

Abstract:

Sodium alginate with different molecular weights (55, 170 and 320 kg.mol<sup>-1</sup>) were chemically modified by grafting methacrylic moieties unto the hydroxyl groups of the alginate backbone. The methacrylation was optimized to obtain different degrees of modification. Under UV light and in presence of a photoinitiator, chemically crosslinked hydrogels were obtained. The swelling behavior and the mechanical properties were seen to be dependent on both the degree of methacrylation and the alginate molecular weight. Due to the chain entanglement present in high viscosity sodium alginate, lower degrees of modification were needed to tune the hydrogels properties. Moreover, in the presence of Ca<sup>2+</sup>, a secondary crosslinking was introduced to the matrix by the coordination of the guluronate moieties with the Ca<sup>2+</sup> ions. Upon dual crosslinking, the hydrogels undergo a fast volume shrinkage leading to a reinforcement of the mechanical properties. The secondary crosslinking was reversible and the hydrogels regained their original shape for at least 3 cycles. In addition, the dual crosslinked network can be used as a mean to induce adhesion between hydrogels as well as a building block for self-folding actuators.

## 1. Introduction

Hydrogels are 3D hydrophilic macromolecular networks with the ability to swell in aqueous media. Smart hydrogels are obtained from the crosslinking of stimuli responsive polymers (Shi *et al.*, 2019). After crosslinking, the stimuli-sensitive property of the precursor (LCST, UCST, sol-gel....) that defines its solubility in water can be triggered by an external stimulus that controls the swelling/shrinking behavior of the hydrogels. The external stimulus can vary from temperature, pH, ionic strength, light, magnetic or even electrical field (Kopeček & Yang, 2007). The crosslinked network can be obtained by either chemical or physical crosslinking. Chemical crosslinking results in a permanent hydrogel

whereas physical crosslinking can be reversible thus allowing a certain control over the resulting crosslinking effect.

Polysaccharides, like cellulose, starch, chitosan, alginate, agarose, are naturally occurring polymer chains extracted from natural resources. These natural polymers show sufficient biocompatibility allowing their use in biomedical applications such as wound dressing, tissue engineering, drug delivery etc ( Conzatti *et al.*, 2019; Luo *et al.*, 2021,). These polymers are naturally abundant, can be relatively easily chemically modified and for the most part of them have high affinity for water thus avoiding the use of toxic organic solvents for processing. However, due to their various structural heterogeneities, it is important to understand the structure-properties relationship in order to control and adapt the different properties for the desired application.

Sodium alginate is a commonly used polysaccharide in the biomedical field. In addition, it has a unique property to complex/coordinate with multivalent cations such as  $\text{Fe}^{3+}$ ,  $\text{Cu}^{2+}$ ,  $\text{Ca}^{2+}$ ,  $\text{Mn}^{2+}$  leading to the formation of physically crosslinked hydrogels (Haug & Smidsrod, 1965; Gamella *et al.*, 2017; Ouwerx *et al.*, 1998; Scheja *et al.*, 2017) . However, alginate physical hydrogels demonstrate weak stability in physiological media leading to the dissociation of the matrix due to the  $\text{Na}^+$  -  $\text{Ca}^{2+}$  ion exchange (Lee & Mooney, 2012). In the literature, stable chemical crosslinking of alginate can be obtained via photo-crosslinking after introduction of methacrylate moieties to the hydroxyl or carboxyl groups present on the backbone (Li *et al.*, 2016). However, despite the stable network generated, the photo-crosslinked hydrogels show weak mechanical properties which can be slightly improved by modifying the methacrylation degree. Tuning the swelling and mechanical properties of sugar-based hydrogels can also be tuned by the introduction of a secondary crosslinking to the polymer network (Hachet *et al.*, 2012; Mihaila *et al.*, 2013; Paepe *et al.*, 2002; Sahraro *et al.*, 2018; Zanon *et al.*, 2022). Early researches combining chemical and ionic crosslinking of alginate were done to improve the performance and properties of microspheres (Fenn *et al.*, 2016; Mahou *et al.*, 2015). Kim *et al.* (Kim *et al.*, 2020) obtained chemically crosslinked alginate hydrogels after functionalizing the carboxyl group with tyramine hydrochloride to allow photo-crosslinking and reinforced the mechanical performance of the matrix by the introduction of calcium ions. Upon dual crosslinking, the water uptake of their hydrogels decreased by 30%. Nevertheless, as the number of free carboxyl groups available to complex with calcium ions decreases due to the functionalization, the complexation with calcium ions is low. Similarly, Gao *et al.* (Y. Gao & Jin, 2019) prepared dual-crosslinked alginate fibers using a microfluidic fabrication system. The dual crosslinked network enhanced the tensile strength of the fibers and improved their stability in physiological conditions compared to physically crosslinked alginate networks. Fenn *et al.* (Fenn *et al.*, 2016) used dual crosslinking on alginate beads to control the release of doxorubicin hydrochloride as a controlled

drug delivery system. They found that dual crosslinking might not be beneficial for the drug encapsulation efficiency due to the entrapment of the drug inside the dual crosslinked network.

These previously cited literature lacks information on the alginate's structural properties such as the molecular weight  $M_w$  and/or monomer composition (Guluronic/Mannuronic ratio) in relation to the structure-property relationship for dual crosslinked alginate hydrogels. In this work, three Alg- $\text{Na}^+$  having a similar G/M ratio but different molecular weights were chemically modified in order to obtain chemically crosslinking networks. Then we investigated the influence of both different degrees of modification and the reversible physical crosslinking on the network's properties. The swelling behavior as well as the mechanical properties were assessed in both water and PBS. In addition, dual crosslinking was used as a mean to induce self-healing and to prepare self-folding actuators with specific shape deformation.

## 2. Materials and methods

### 2.1. Materials

Sodium alginate (Alg- $\text{Na}^+$ ) medium (MVA) and high viscosity (HVA) having G/M = 0.6 - 0.7 were generously donated by Algaia (Saint Lo, FRANCE). Low viscosity sodium alginate (LVA) was purchased from Sigma-Aldrich. The samples characterization can be found in the supplementary information (Figure S1 & Table S1). Methacrylic anhydride (MA), calcium chloride ( $\text{CaCl}_2$ ), ethylenediaminetetraacetic acid tetrasodium salt dihydrate ( $\text{EDTA } 4\text{Na}^+ , 2\text{H}_2\text{O}$ ) and phosphate buffered saline (PBS) were purchased from Sigma-Aldrich. Triethylamine (TEA) was purchased from Fisher Chemicals. Milli-Q water (conductivity = 18.2  $\text{m}\Omega\cdot\text{cm}$  at 23°C) was used during this study. Lithium phenyl-2,4,6-trimethylbenzoylphosphinate (LAP) was synthesized as described by Maima *et al.* All chemicals were used without further purification unless mentioned otherwise.

### 2.2. Methods

#### *Sodium alginate chemical modification*

Methacrylated alginate (Alg-MA) was obtained by reacting Alg- $\text{Na}^+$  with methacrylic anhydride (MA). A 2 wt/v% aqueous Alg- $\text{Na}^+$  was prepared by dissolving 1 g of sodium alginate in 50 mL milli-q water in a 250 mL round bottom flask under magnetic stirring (700 rpm). In order to obtain a homogeneous mixture, the solution was left to stir for 4 hours. TEA was then added at different molar equivalent with respect to MA and the solution was left to stir for 30 minutes to ensure complete homogenization. Finally, MA was added at different molar equivalents with respect to the sugar unit. The reaction was maintained at 24°C for 24 hours. Functionalized Alg- $\text{Na}^+$  was obtained by precipitating the mixture in cold acetone followed by drying at 24°C under reduced pressure.

Different degrees of methacrylation were obtained by varying the amount of MA or TEA:MA added as summarized in table S1. The functionalized alginate will be denoted by LVAx, MVAx or HVAx where LVA, MVA and HVA represents low viscosity alginate (54 000 g.mol<sup>-1</sup>), medium viscosity alginate (170 000 g.mol<sup>-1</sup>) and high viscosity alginate (320 000 g.mol<sup>-1</sup>) respectively and x the degree of modification by methacrylate moieties per sugar unit (in %).

#### *<sup>1</sup>H NMR characterization*

In order to quantify the degree of modification (DM), <sup>1</sup>H NMR was used. 20 mg of Alg-MA was dissolved in 1mL D<sub>2</sub>O and left to stir for 1 hours to obtain a homogeneous mixture. The <sup>1</sup>H NMR spectra were recorded on a Bruker Avance I 400 MHz (64 scans, 5 s relaxation time). The DM, defined as the number of methacrylates per sugar moiety, was calculated as the ratio of the protons of methacrylate (1.95 ppm, 5.8 ppm and 6.2 ppm) and H<sub>G1</sub> proton of the alginate using the following equation.

$$DM (\%) = G\% * \frac{I_{H \text{ vinyl } 6.2 \text{ ppm}}}{I_{H_G \text{ } 5 \text{ ppm}}} \quad (\text{Equation 1})$$

Where I<sub>H</sub> represents the intensity of a vinyl protons of the grafted methacrylate at 6.2ppm, I<sub>H<sub>G1</sub></sub> represents the intensity of the anomeric protons of the guluronic moieties and G% represents the fraction of guluronic units in the polysaccharide. The G% is calculated by comparing the anomeric G proton at 5.8 ppm with the anomeric M proton at 4.47ppm.

#### *Hydrogel preparation*

The photo-crosslinkable aqueous alginate resin consists of 3 wt/v% Alg-MA and 0.1125 wt/v% LAP as photo-initiator. The alginate resin was injected in a cylindrical Teflon mold (1 cm diameter and 4 mm thickness), covered with a glass slide to ensure a flat surface and avoid solvent evaporation and photo-crosslinked under UV (365 nm) for 20 minutes using a UV Crosslinker Bio-Link chamber (Thermo Fischer, France) at 2-3 mW.cm<sup>-2</sup>. Before the swelling/mechanical assays, the hydrogels were left to swell in water for 8 hours (changing the water twice) to ensure the removal of all unreacted species. Then, they were dried on a Teflon sheet in a 45°C oven for 24 hours until reaching a constant weight.

#### *Gel content (GC)*

For this study hydrogels were used directly after UV curing. Upon photo-crosslinking, the hydrogels were dried on Teflon sheet in a 45°C oven for 24 hours until constant weight. The dry mass was recorded and denoted by m<sub>dry 1</sub>. The hydrogel was then left to swell in water for 24 hours (changing the water twice) followed by oven drying. The mass of the dry washed hydrogels was recorded and denoted m<sub>dry 2</sub>. The gel content (GC) was calculated using the following equation (Jalil *et al.*, 2017).

$$GC = 100 * \frac{m_{dry 2}}{m_{dry 1}} \quad (\text{Equation 2})$$

### *Swelling kinetics*

To follow the swelling kinetics of the hydrogels in water, a washed dry hydrogel disk was placed in 40 mL Milli-Q water. The hydrogel was then weighted at different time intervals after removing the excess water with a wet KimTech paper. Between measurements, the gel was left to swell in a  $24 \pm 1$  °C room. The swelling degree (Q) was calculated using the following equation.

$$Q = \frac{m_{swollen \text{ at time } t}}{m_{dry}} \quad (\text{Equation 3})$$

### *Cyclic swelling*

The equilibrium cyclic swelling degrees were measured starting from the washed dry hydrogels. The cycles were water  $\rightarrow$  10 wt/v% aq CaCl<sub>2</sub>  $\leftrightarrow$  1 wt/v% aq EDTA and PBS  $\leftrightarrow$  10 wt/v% to mimic physiological conditions. For each measurement, the hydrogel was left to swell for 24h in a  $24 \pm 1$  °C room. The swelling degree was calculated using equation 2. The values are represented as the mean of triplicate sets. The standard deviation was found to be around 20% for each value. The error bars are not shown on the figures to avoid their superposition and maintain a lucid reading.

### *Compression testing*

Compression tests of the swollen hydrogels were executed on an Instron 3366L5885 mechanical tester equipped with a 100N load cell. Cylindrical samples of 10 × 4 mm were prepared in a Teflon mold as previously described, washed, dried then left to swell in water. Hydrogels were taken at different points of the cycling swelling and the compression tests were done after measuring the dimensions using a caliper. The compression speed was set at 1 mm.s<sup>-1</sup> with 200 ms sampling time. Each value is represented by the mean  $\pm$  SD (n = 3). The Young's modulus was as the slope at 3% deformation.

### *Induced self-healing*

The threshold for the successful induced self-healing was determined using washed dry hydrogels. The hydrogels were left to swell in water for different time intervals to vary the swelling degree. It was then cut in half, rearranged in the desired architecture and glued with few microliters of 10wt/v% aqueous CaCl<sub>2</sub> solution. Calcium was left to diffuse for 30 seconds before manually extending the hydrogel to test its stability.

### *Actuator preparation*

Alginate-based actuators were first built by creating a dual-crosslinking gradient. The gradient was obtained by calcium diffusion from the top surface of the hydrogel for 5s. Before curing, the

methacrylated alginate resin was placed in 30x15 mm mold with thicknesses of 0.5, 0.75 and 1 mm. On the surface of the resin, calcium was left to diffuse for 5 s by applying a wet filter paper with 5 w/v CaCl<sub>2</sub>. Afterwards, the surface of the mold was covered with a glass slide to ensure a flat surface and avoid water evaporation and then photo-crosslinked under UV (365 nm) for 20 minutes.

Secondly, hydrogel films were patterned in order to obtain alternating chemically and dual-crosslinked section. In order to do so, alginate resin containing LAP as photo-initiator was firstly introduced in a 25x10x1 mm PDMS mold. Then, physical crosslinking was patterned on the surface of the film using a filter paper dipped in CaCl<sub>2</sub> solution. Following the physical crosslinking pattern, the PDMS mold was covered with a glass slide and then cured under UV (365 nm) light for 20 minutes.

After curing, the hydrogels were left to swell in water for 3 hours to ensure that the equilibrium swelling degree was reached.

### **3. Results and discussion**

#### **3.1. Sodium alginate chemical modification**

The addition of photo-sensitive function on the alginate's backbone provides the ability to obtain a chemically crosslinked network under UV irradiation and in the presence of a photo-initiator. The common method of functionalization is by grafting methacrylate groups on the hydroxyl or carboxyl of the polysaccharides' unit (Luo *et al.*, 2021). The reaction commonly occurs in the presence of methacrylic anhydride, glycidyl methacrylate, 2-aminoethyl methacrylate or by microwave assisted methacrylation (İlhan *et al.*, 2020; Zanon *et al.*, 2022). Reaction conditions requires either careful control of pH with concentrated NaOH, very long reaction times to favor ring opening over the transesterification reaction, the use of organic cosolvent or complex apparatus with careful temperature control (İlhan *et al.*, 2020). Herein, the methacrylation is done in water, in the presence of excess of triethylamine (TEA) (mild basic conditions) and methacrylic anhydride (MA) and for 24 hours in an ice bath during the first four hours. The methacrylation will be done on three batches of sodium alginate having various molecular weights as obtained by GPC (Table S2); low viscosity alginate (54 000 g.mol<sup>-1</sup>) denoted as LVA, medium viscosity alginate (170 000 g.mol<sup>-1</sup>) denoted MVA and high viscosity alginate (320 000 g.mol<sup>-1</sup>) denoted HVA. For a fixed concentration in water, increasing the molecular weight of the alginate backbone will result in an increase of the viscosity of the solution (figure S4) because of the formation of notable chain entanglements hence the nomenclature chosen.

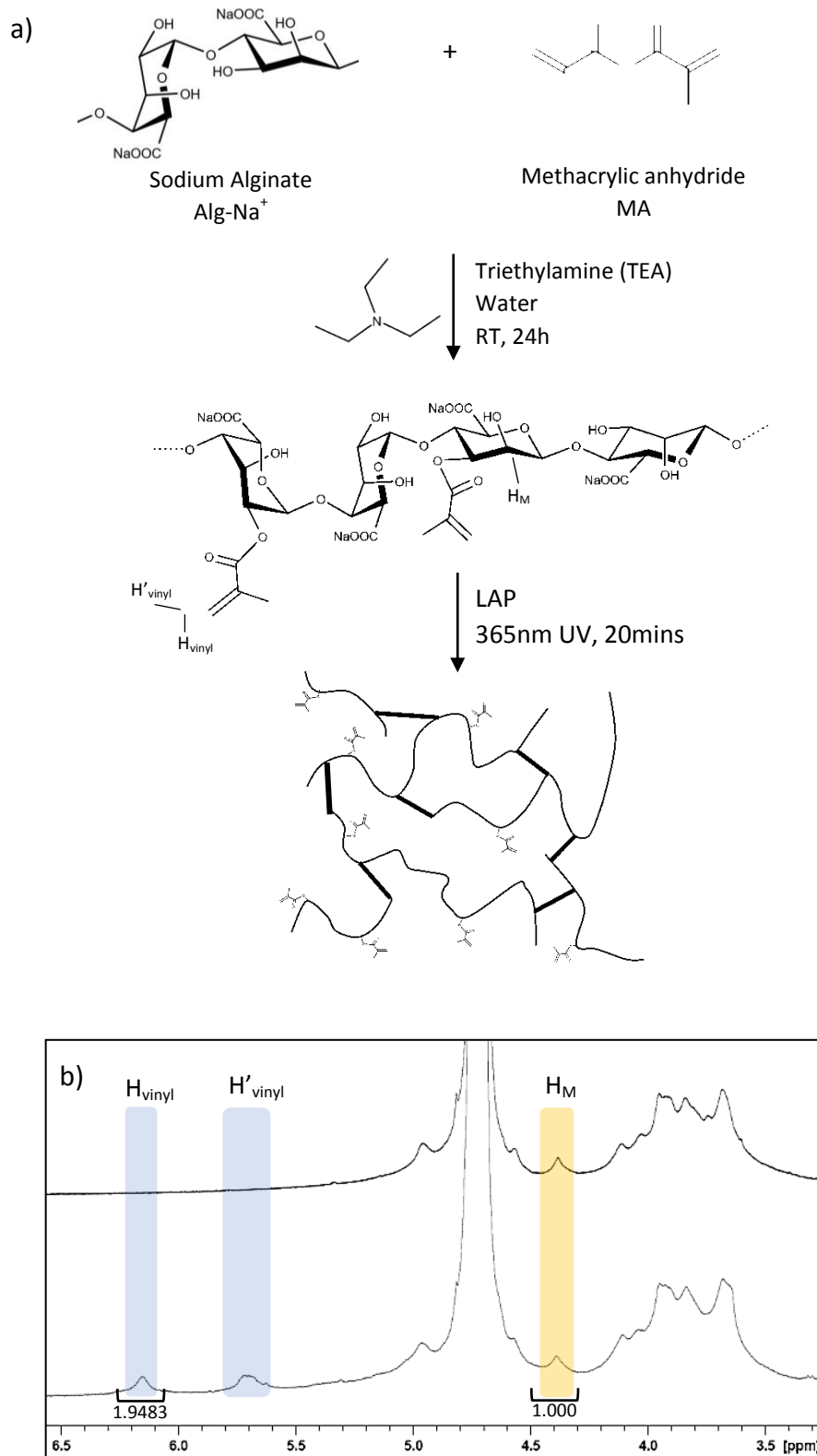


Figure 1. a) Schematic illustration of the methacrylation of sodium alginate and its photo-crosslinking and b) NMR spectra of native MVA (top) and methacrylated MVA80 (bottom).



In order to obtain the photo-crosslinkable sodium alginate resin, methacrylic moieties were grafted on the alginate backbone by reacting the hydroxyl groups with methacrylic anhydride as shown in figure 1. By grafting the methacrylic moieties on the hydroxyl groups, the carboxylic acids remain available to coordinate with  $\text{Ca}^{2+}$  and which then can be used to provide a secondary reversible crosslinking in the hydrogel matrix (Schweiger, 1962). During methacrylation, methacrylic acid will be released as a byproduct of the reaction or as a result of the hydrolysis of the methacrylic anhydride. In order to avoid drastic drop in pH, which will cause the formation of alginic acid and its precipitation (Lee & Mooney, 2012), TEA was used as a poor nucleophilic base in order to neutralize the acids formed while preventing the hydrolysis of the formed esters.

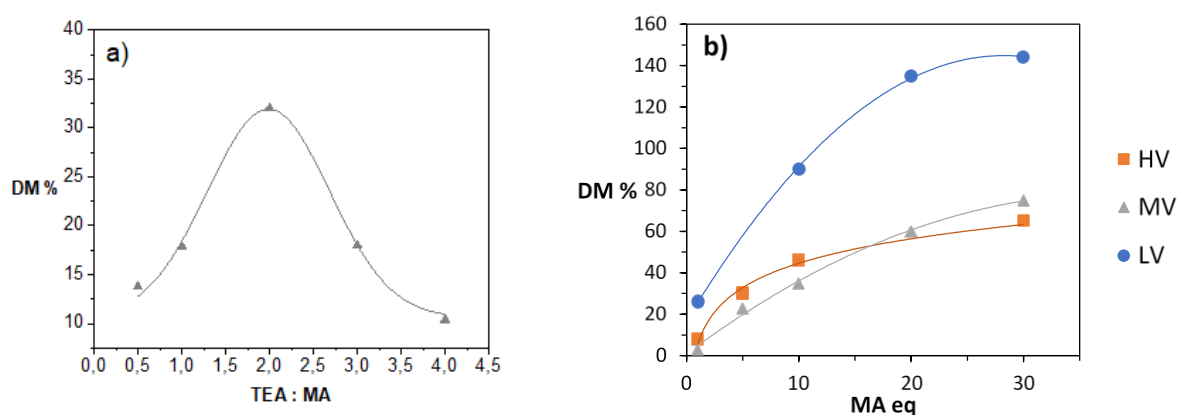


Figure 2. Influence of a) TEA/MA ratio for a fixed MA = 10eq on the DM of MVA and b) MA equivalence for a fixed TEA/MA = 2 eq on the DM of LVA, MVA and HVA.

The successful methacrylation can be observed on the  $^1\text{H}$  NMR spectra as shown in figure S1. The vinyl protons of the grafted methacrylates appear at 5.8 and 6.2ppm while the methyl protons appear at 1.9ppm. Two main parameters were seen to influence the DM as observed in figure 2: the molar ratio TEA/MA and the equivalent of MA added. For MV alginate, increasing TEA/MA molar ratio, the DM increases until a peak of 33% is reached at TEA/MA = 2eq, it then decreases afterwards to 10% for 4eq TEA. At low TEA/MA molar ratio, not enough TEA is present to neutralize the methacrylic acids formed. A drop in pH is observed causing an increase in the viscosity due to hydrogen bonding between the protonated carboxylic acid which limits the MA and hydroxyl groups access leading to lower DM. At TEA/MA  $\geq$  2, triethylamine will catalyze the hydrolysis of the anhydride compared to nucleophilic acyl substitution reaction (Cooper *et al.*, 2017) favoring the formation of methacrylic acid rather than grafting on the alginate backbone leading to lower DM. In addition, increasing the added MA will yield higher DM while hydrolysis occurs. A logarithmic increase is observed until a plateau is achieved due to the steric hindrance caused by the grafted

methacrylic moieties (Gerola *et al.*, 2016; Zanon *et al.*, 2022). The same tendency is observed for the low viscosity sodium alginate ( $54\ 000\ \text{kg}\cdot\text{mol}^{-1}$ ) but with higher DM values. In fact, decreasing the molecular weight of alginate will increase the number of hydroxyl groups present at the chain ends thus increasing the reactive sites for the methacrylation to occur and allows for a lower viscosity of the reaction medium favoring a more homogeneous methacrylation.

### 3.2. Photo crosslinking of methacrylated alginate

Alginate-based hydrogels are commonly obtained *via* the physical crosslinking of the polysaccharide with  $\text{Ca}^{2+}$  (X. Gao *et al.*, 2018; Kuo & Ma, 2008; Ouwerx *et al.*, 1998). These ionically crosslinked hydrogels have weak stability in physiological media thus limiting their applications in the biomedical field (Lee & Mooney, 2012). Chemical crosslinking provides the formation of a stable matrix where the ionic crosslinking can be used as a mean to tune the hydrogel's properties.

The hydrogels were prepared by photo-polymerization of the functionalized alginate in presence of lithium phenyl-2,4,6-trimethylbenzoylphosphinate (LAP) as photo-initiator under UV light. The amount of LAP as well as irradiation time were optimized as represented in figure S2-S3. Alginate with different molecular weights and various degrees of methacrylation were used in order to study the influence of these parameters. The weight percentage of Alg-MA and LAP were kept at 3 w/v% and 3.75 w/w% respectively. To form the crosslinked network, Alg-MA underwent free radical polymerization under UV light to form crosslinking bridges between the methacrylate groups. The hydrogels obtained upon crosslinking have various physical aspects, from soft and elastic to hard and brittle depending on the degree of modification.

The gel content, defined as the percentage of Alg-MA present in the crosslinked matrix after washing, was seen to be dependent on both the alginate molecular weight and the degree of modification. As seen in figure 3, increasing the alginate molecular weight and/or the degree of crosslinking will increase the gel content of the hydrogels. For example, for sodium alginate having a Mw of  $170\ 000\ \text{g}\cdot\text{mol}^{-1}$  (MVA), increasing the DM from 20 to 60% will increase the gel content from 60 to 90%. The presence of more methacrylate moieties on the alginate backbone will improve the formation of interchain bridges between the methacrylate groups to obtain a crosslinked network. Moreover, for low molecular weight Alg- $\text{Na}^+$ , higher DM is needed to achieve important gel contents. For a  $54\ 000\ \text{g}\cdot\text{mol}^{-1}$  Alg- $\text{Na}^+$  (LVA), at DM 90%, the GC is around 70%, compared to Alg- $\text{Na}^+$  of  $320\ 000\ \text{g}\cdot\text{mol}^{-1}$  (HVA) where the GC reaches 92% for 75% degree of modification. In fact, for high molecular weight alginates a lower degree of modification is needed to crosslink due to the increase in chain entanglements providing additional physical crosslinking. Chain entanglements are dependent on the backbone's molecular weight (Figure S4, Table S3). Increasing the molecular

weight of the sodium alginate will result in a decrease of the critical entanglement concentration which help to obtain a stable chemical network even with low DM.

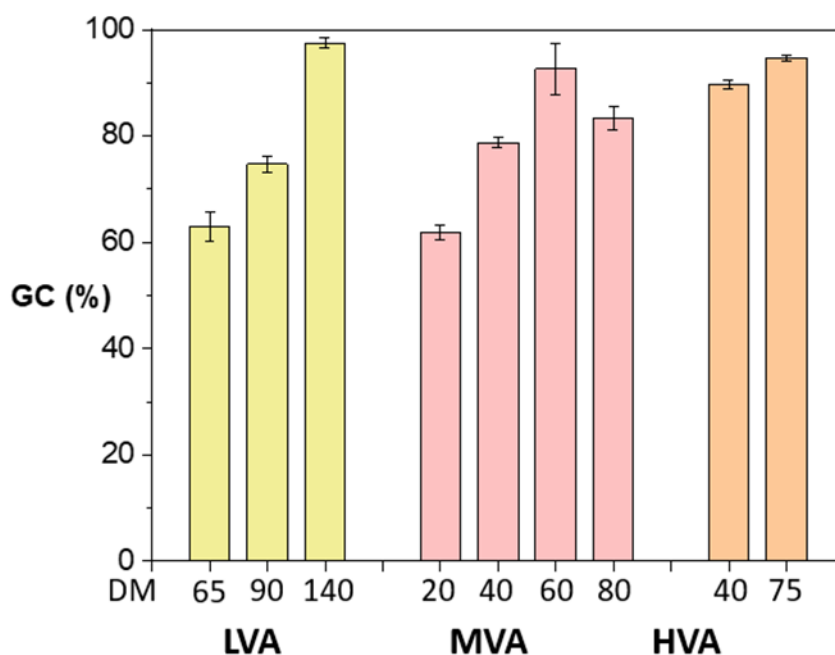


Figure 3. Gel content of the hydrogels as function of the Alg Mw and DM.

### 3.3. Cyclic shape morphing of alginate hydrogels

To investigate the influence of the crosslinking density on the hydrogels swelling ability; the swelling degree of hydrogels with various methacrylated alginate were determined at different conditions. First, the swelling behavior of the chemically crosslinked hydrogels was determined in water for 24h even though the equilibrium is reached in 1 hour (figure S5). Second, additional crosslinking was introduced to the chemically crosslinked network upon submerging in a  $\text{CaCl}_2$  solution where the water uptake of the dual crosslinked network was measured. The secondary ionic crosslinking is reversible upon submerging the hydrogels in an EDTA-rich solution. EDTA is a  $\text{Ca}^{2+}$  chelating molecule which extracts the calcium ions from the alginate hydrogels. To better understand the behavior of the system in physiological conditions, the cyclic swelling was also studied between PBS and 10 wt/v% aqueous  $\text{CaCl}_2$ . PBS also plays the role of a calcium decomplexing agent due to the  $\text{Na}^+ - \text{Ca}^{2+}$  ion exchange (Zhao *et al.*, 2014).

As seen in figure 4, upon submerging the chemically crosslinked hydrogels in water the hydrogels swell at significantly different swelling degrees. It can be seen that both the DM and alginate molecular weight directly influence the swelling degree. In fact, in water, increasing the DM will decrease the water uptake due to a higher degree of crosslinking. For example, increasing the DM of

MVA ( $170\,000\text{ g}\cdot\text{mol}^{-1}$ ) from 40 to 80% will decrease the swelling ratio from 160 to 50. Higher DM will result in a higher degree of crosslinking of the matrix which then limits its water uptake capacity. Moreover, for LVA ( $54\,000\text{ g}\cdot\text{mol}^{-1}$ ), higher degrees of crosslinking are needed to drastically tune the swelling behavior. For example, increasing the DM from 55% to 140% will lead to a decrease of the water uptake from 115 to 30. For similar degrees of methacrylation, increasing the sodium alginate molecular weights yields lower swelling degrees which can be explained by the increase in chain entanglements when having longer polysaccharide chains. For instance, LVA60 has a significantly higher swelling degree than MVA60 of 130 compared to 80 respectively. This influence of the degree of methacrylation and the alginate molecular weight on the hydrogel matrix can also be confirmed by comparing the mesh sizes by rheology (Table S6). The same tendency is observed for HVA ( $320\,000\text{ g}\cdot\text{mol}^{-1}$ ) hydrogels, however hydrogels with lower DM could not be obtained due to the fragility of the hydrogels. The same correlation between the DM and alginate -molecular weight is observed in PBS. It is important to note that the swelling capacity in PBS is lower than in water and that is due to the higher ionic strength of the solution (Bajpai & Johnson, 2005; Drozdov & Christiansen, 2015; Roy *et al.*, 2011). In the presence of salt rich media, the negatively charged alginate backbone interacts with the positively charged counterions limiting the repulsion force between the  $-\text{COO}^-$  thus leading to lower swelling degrees.

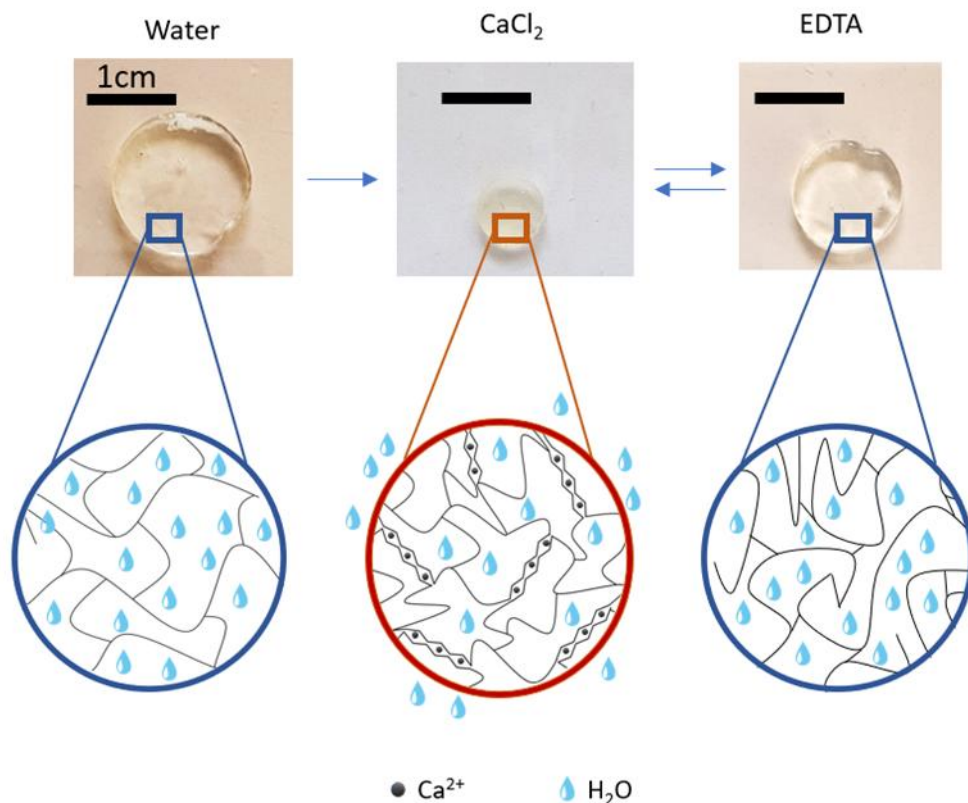


Figure 4. Physical and schematical illustration of the cycling shape morphing of MVA40 in water.

The secondary crosslinking was introduced into the matrix after immersing the swollen hydrogels in a  $\text{CaCl}_2$  solution where the swelling degree drastically drop. When the hydrogels are surrounded by  $\text{Ca}^{2+}$  rich solution, the calcium will diffuse inside the hydrogel's matrix and will coordinate between the free carboxylic acids of guluronate moieties bringing the chains closer to each other. This secondary crosslinking expels the water from the matrix translated by the shrinking of the hydrogels by more than two times their original dimensions as seen in figure 4. For LVA ( $54\,000\text{ g.mol}^{-1}$ ) the swelling degree decreases from 120 to 50 and 45 to 10 for DM 60 and 90 respectively upon the addition of the secondary crosslinking as summarized in figure 5a.

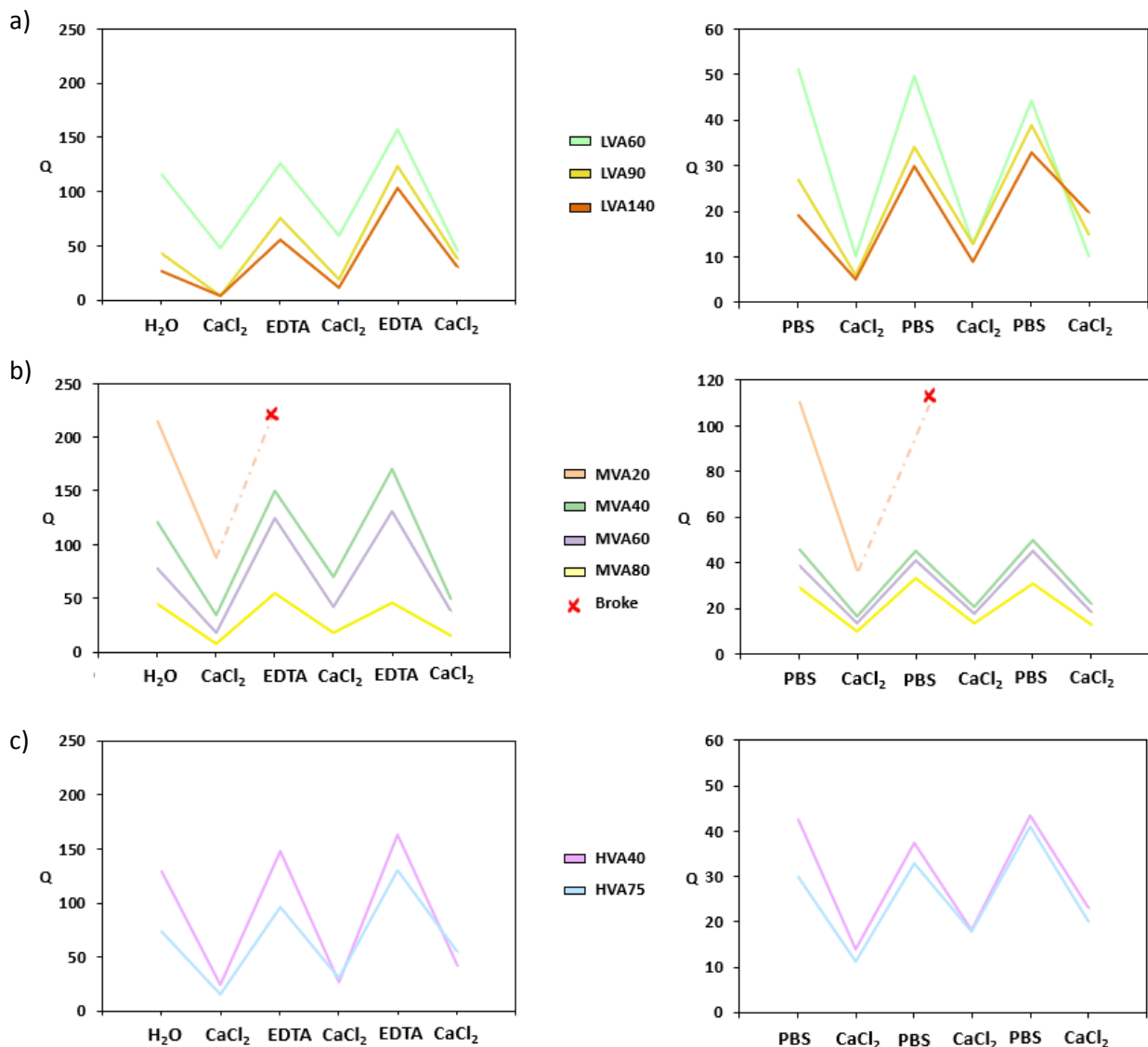


Figure 5. Cyclic swelling behavior of a) LVA b) MVA and c) HVA alginate hydrogels in water and PBS.

The secondary physical crosslinking is reversible in the presence of EDTA as seen in figure 5. In fact, EDTA is a calcium chelating agent with a stronger affinity to calcium than sodium alginate. Hence, in

the presence of an EDTA rich solution, calcium ions will be extracted from the dual-crosslinking hydrogels reversing the physical crosslinking. Upon extraction, water will re-diffuse into the matrix and the hydrogels regain their initial swelling degree and shape. The swelling/shrinking behavior was seen to be reversible for at least 3 cycles.

### **3.4. Influence of dual crosslinking on the mechanical properties**

One of the main advantages of chemically crosslinked networks is the ability to tune the mechanical properties by modifying the degree of crosslinking (Jeon *et al.*, 2007). As previously seen, the swelling behavior is directly affected by the DM. The same correlation can be extrapolated to the mechanical properties. The mechanical behavior of the hydrogels was studied by compression tests.

By increasing the degree of methacrylation from 60 to 140 for LVA ( $54\ 000\ \text{g}\cdot\text{mol}^{-1}$ ), the compression modulus in water increases from 0.047 to 0.524 MPa. This increase is due to the higher degree of crosslinking forming a tighter network correlated with the decrease of the water uptake. The same tendency is also observed for the MVA ( $170\ 000\ \text{g}\cdot\text{mol}^{-1}$ ) and HVA ( $320\ 000\ \text{g}\cdot\text{mol}^{-1}$ ) hydrogels (Figure 6). The impact of chain entanglements can also be seen in the mechanical properties, where the compression modulus of HVA75 hydrogel of 0.182 MPa which is higher than LVA90. Hence, the mechanical properties of the hydrogels can be tuned by either modifying the degree of methacrylation or the molecular weight of the alginate. Furthermore, the introduction of a secondary crosslinking by calcium ions drastically improves the compression modulus by up to 100 times. Upon the formation of additional crosslinking bridges, the hydrogels collapse resulting in a much denser network. For example, as seen in figure 6 the compression modulus of MVA40 increases from 0.004 MPa to 2.5 MPa. The improvement is also seen for the other hydrogels when having dual-crosslinked hydrogels. Finally, upon extracting calcium ions from the system with EDTA, the compression modulus decreases as the hydrogels re-swells. The reversibility of the reinforcement of the mechanical properties by the addition of calcium ions was also observed for the hydrogels previously swollen in PBS.

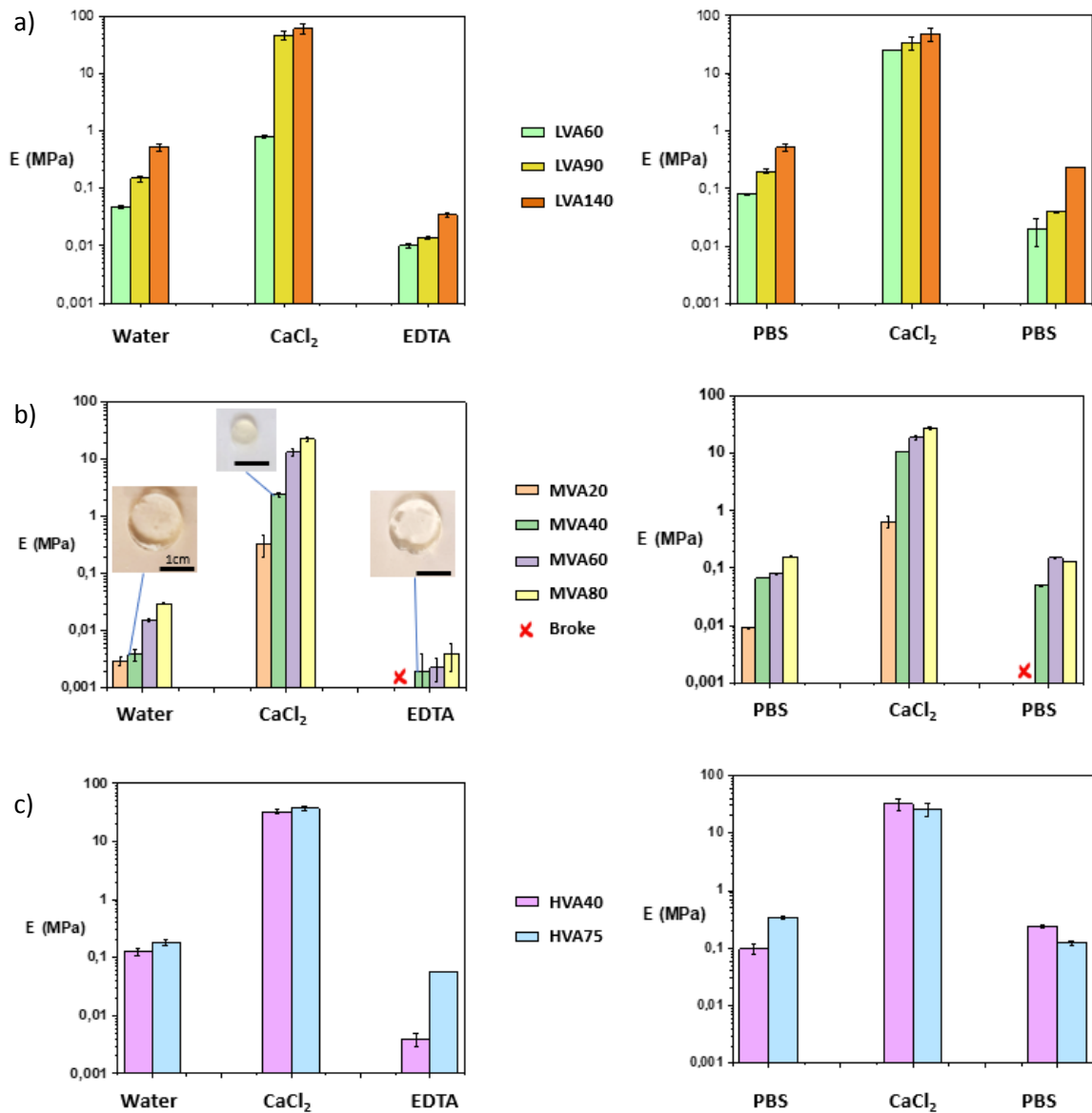
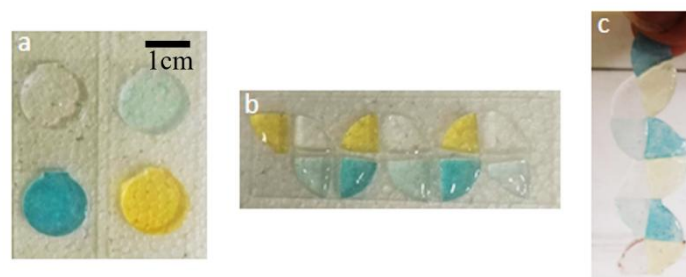


Figure 6. Compression modulus a) LVA b) MVA and c) HVA alginate hydrogels in water and PBS at different points of the cycling swelling.

### 3.5. Ion induced self-healing

We have demonstrated the promising dual crosslinking approach to not only reinforce the mechanical properties of the hydrogel but also to modify the volume of the hydrogel by controlled water absorption/desorption. In addition, dual crosslinking can also be used to induce self-healing/auto assembly. The ionic crosslinking can be used as a tool to repair/adhere hydrogels together (Wei *et al.*, 2013). By simply cutting the hydrogel MVA60 and rearranging the pieces to the

desired architecture, few drops of  $\text{CaCl}_2$  can be used to induce self-healing at the interface of the cut pieces as represented in figure 7. Four cylindrical hydrogels can be cut in pieces and rearranged to obtain a snake-like structure. However, it was observed that the induced self-healing is limited by a certain swelling threshold. It was seen that the healed part of the hydrogel is stable up until a certain threshold. In other words, the induced self-healing ability dissociate at a certain water uptake which can be explained by the intense stress created at the interface of the healed part. The stress induced from the swelling of the hydrogel is stronger than the physical interactions that holds the hydrogel together. In addition, it was also observed that the induced self-healing is more efficient at lower water uptake ratios. At low swelling capacities, the polymer chains are closer to each other which facilitates the coordination between two separate carboxylic groups of two different chains. The limiting swelling degree above which the induced healing does not work anymore was found to be around 30 across all samples. This can be used as a tool to control the release of parts of the hydrogel in order to control its shape throughout time.



*Figure 7. Induced self healing used to transform MVA60 hydrogels from disk-shape structures to a snake-like architecture.*

### **3.6. Controlled dual crosslinking as an actuating mechanism**

Hydrogel actuators are mainly built by combining one layer with a high swelling degree with another showing little volume change (Han *et al.*, 2020; L. Wang *et al.*, 2018). The anisotropic swelling behavior in the bilayer system creates mechanical stresses at the interface of the layer forcing the system to bend. Bilayer hydrogel actuators are limited by the stability of the adhesion between the two layers. Stable systems can be obtained by a two steps polymerization where one layer is cured on top of the other, phase separation or the use of glue. For each method, the chemistry of each layer should be carefully selected to ensure a strong interpenetrating network which then remains a limitation. Alginate-based actuators are mainly studied under an electrochemical stimulus where the deformation is governed by the movement of the ions in the hydrogels (Jia *et al.*, 2023; Lv *et al.*,



2022). Upon the induction of an electric current, an electric field will be created between the electrodes where the hydrogel is placed. The ions will move accordingly inducing a shape deformation.

As previously described, the significant difference in the swelling degree between the chemically crosslinked alginate network and the dual-crosslinked one can also be used as a mean to induce shape deformation. On the first hand, a dual-crosslinking gradient was obtained by the calcium diffusion from the top surface of the hydrogel films. Compared to bilayer system, by creating a swelling gradient in the system there is no possible delamination of the layers. Several self-folding actuators were obtained using LVA90 by varying the thickness of the hydrogel film (0.5 mm, 0.7 mm and 1 mm) and maintaining the same calcium diffusion time. The diffusion time was fixed at 5 s using a wet filter paper with a 5 w/v% CaCl<sub>2</sub> solution to obtain a dual-crosslinking gradient; more than 5 s will result in the full dual crosslinking of the hydrogels where no shape deformation was observed. The dual-crosslinking gradient across the hydrogel will create an anisotropic swelling degree in the hydrogels resulting the bending of the system towards the denser dual-crosslinked section. As illustrated in figure 8, upon submerging in water, several tube diameters can be obtained ranging from 2.7mm to 5.5mm, by simply increasing the thickness of the hydrogel. The correlation between the thickness of the hydrogel and the radius of curvature is confirmed by Timoshenko's formula that simulates the deformation of bilayer thermostats used also for bilayer hydrogels (Figure S6) (Timoshenko, 1925; X. Wang *et al.*, 2019).

Moreover, more complex shape deformations can be obtained by patterning the hydrogels (Shang & Theato, 2018). In fact, patterning creates local anisotropic swelling degrees which can result in more complex shape transformations similarly as reported by *Shang et al.* where they induced rolling, twisting or curling deformations based on the pattern's direction on a PNIPAM / PAAc bilayer system. By locally patterning the hydrogel with Ca<sup>2+</sup> to obtain dual-crosslinked alternating regions, specific deformations can be achieved. For example, 45° patterning will result in a helix shape deformation whereas a 90° pattern will result in a tubular shape-like deformation as observed in figure 8.

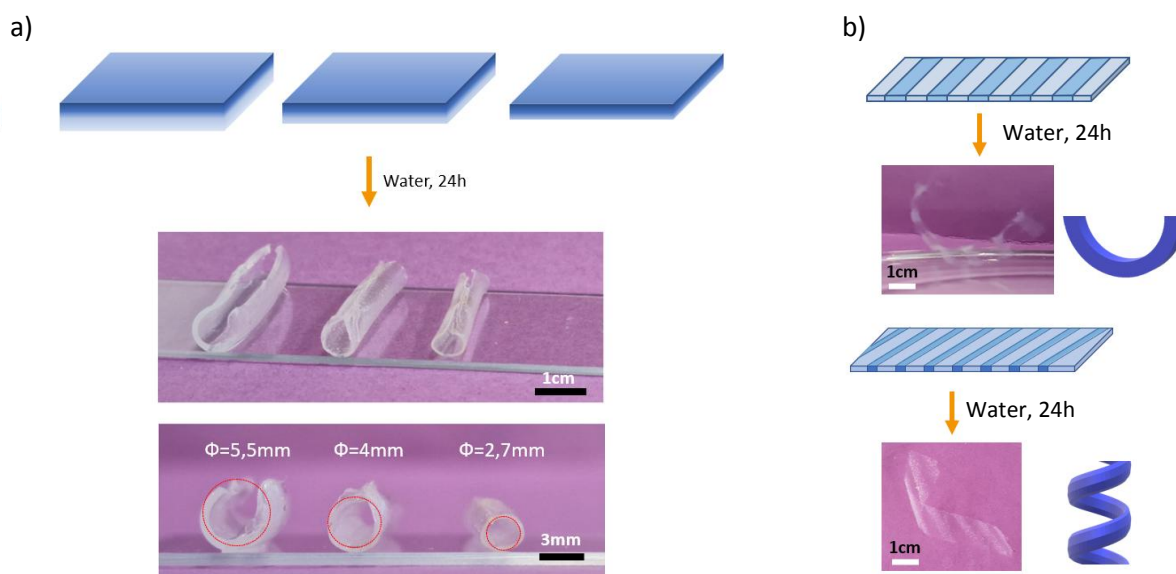


Figure 8. LVA90 hydrogel actuators obtained by a) gradient dual-crosslinking (film thickness 1 mm, 0.7 mm, 0.5 mm from left to right) and b) patterned dual-crosslinking representing curving and helicoidal actuation. The shade blue represents the dual crosslinking.

#### 4. Conclusion

In this study, alginate hydrogels were obtained by chemically modifying sodium alginate with methacrylic anhydride in the presence of TEA under mild conditions. The reaction was optimized to obtain various degrees of methacrylation for sodium alginate of 54, 170 and 320 kg.mol<sup>-1</sup>. By modifying the amount of MA added, several DM were obtained up to 140%, 80% and 75% for LVA (54 000 g/mol<sup>-1</sup>), MVA (170 000 g/mol<sup>-1</sup>) and HVA (320 000 g/mol<sup>-1</sup>) respectively. Afterwards, hydrogels were obtained by photo crosslinking in the presence of LAP as photo-initiator under UV lights. The water uptake and compression modulus were seen to be directly influence by the DM. Increasing the DM will result in a higher degree of crosslinking leading to a lower swelling degree and higher compression modulus. In addition, increasing the molecular of the alginate backbone will reinforce the mechanical properties due to higher chain entanglements. Then, the potential properties that can be induced by the ability of sodium alginate to coordinate with calcium ions were thoroughly investigated. The secondary crosslinking can be used as a tool to tune the swelling uptake, mechanical properties, induce healing as well as shape deformation to chemically crosslinked alginate hydrogels. The secondary physical crosslinking can be used as a tool to improve the mechanical properties of the hydrogels as well as induce important volume changes. In addition, calcium ions can be used to trigger adhesion between two different hydrogel pieces with some limitations. Finally, the significant difference between chemically and dual-crosslinked networks was

used as a mean to induce shape deformation by simple calcium diffusion from the surface. Several self-folding actuators were built to obtain tubes with different diameters when modifying the thickness of the hydrogels. Moreover, complex architecture such as helices can be obtained by patterning the hydrogels at a specific angle. By properly choosing the alginate molecular weight, specific volume changes and shape deformation can be obtained. This study represents progress in understanding the potential physicochemical capabilities of smart biomaterials.

## References

- Bajpai, S. K., & Johnson, S. (2005). Superabsorbent hydrogels for removal of divalent toxic ions. Part I: Synthesis and swelling characterization. *Reactive and Functional Polymers*, 62(3), 271–283. <https://doi.org/10.1016/j.reactfunctpolym.2005.01.002>
- Conzatti, G., Cavalie, S., Gayet, F., Torrisani, J., Carrère, N., & Tourrette, A. (2019). Elaboration of a thermosensitive smart biomaterial: From synthesis to the ex vivo bioadhesion evaluation. *Colloids and Surfaces B: Biointerfaces*, 175, 91–97. <https://doi.org/10.1016/j.colsurfb.2018.11.084>
- Cooper, W. C., Chilukoorie, A., Polam, S., Scott, D., & Wiseman, F. (2017). A comparative study on the hydrolysis of acetic anhydride and N,N-dimethylformamide: Kinetic isotope effect, transition-state structure, polarity, and solvent effect. *Journal of Physical Organic Chemistry*, 30(12), e3701. <https://doi.org/10.1002/poc.3701>
- Drozдов, A. D., & Christiansen, J. deClaville. (2015). Modeling the effects of pH and ionic strength on swelling of anionic polyelectrolyte gels. *Modelling and Simulation in Materials Science and Engineering*, 23(5), 055005. <https://doi.org/10.1088/0965-0393/23/5/055005>
- Fenn, S. L., Miao, T., Scherrer, R. M., & Floreani, R. A. (2016). Dual-Cross-Linked Methacrylated Alginate Sub-Microspheres for Intracellular Chemotherapeutic Delivery. *ACS Applied Materials & Interfaces*, 8(28), 17775–17783. <https://doi.org/10.1021/acsami.6b03245>
- Gamella, M., Privman, M., Bakshi, S., Melman, A., & Katz, E. (2017). DNA Release from Fe<sup>3+</sup>-Cross-Linked Alginate Films Triggered by Logically Processed Biomolecular Signals:

- Integration of Biomolecular Computing and Actuation. *ChemPhysChem*, 18(13), 1811–1821.  
<https://doi.org/10.1002/cphc.201700301>
- Gao, X., Zhang, Y., & Zhao, Y. (2018). Zinc oxide templating of porous alginate beads for the recovery of gold ions. *Carbohydrate Polymers*, 200, 297–304.  
<https://doi.org/10.1016/j.carbpol.2018.07.097>
- Gao, Y., & Jin, X. (2019). Dual Crosslinked Methacrylated Alginate Hydrogel Micron Fibers and Tissue Constructs for Cell Biology. *Marine Drugs*, 17(10), 557. <https://doi.org/10.3390/md17100557>
- Gerola, A. P., Silva, D. C., Matsushita, A. F. Y., Borges, O., Rubira, A. F., Muniz, E. C., & Valente, A. J. M. (2016). The effect of methacrylation on the behavior of Gum Arabic as pH-responsive matrix for colon-specific drug delivery. *European Polymer Journal*, 78, 326–339.  
<https://doi.org/10.1016/j.eurpolymj.2016.03.041>
- Hachet, E., Van Den Berghe, H., Bayma, E., Block, M. R., & Auzély-Velty, R. (2012). Design of Biomimetic Cell-Interactive Substrates Using Hyaluronic Acid Hydrogels with Tunable Mechanical Properties. *Biomacromolecules*, 13(6), 1818–1827.  
<https://doi.org/10.1021/bm300324m>
- Han, Z., Wang, P., Mao, G., Yin, T., Zhong, D., Yiming, B., Hu, X., Jia, Z., Nian, G., Qu, S., & Yang, W. (2020). Dual pH-Responsive Hydrogel Actuator for Lipophilic Drug Delivery. *ACS Applied Materials & Interfaces*, 12(10), 12010–12017. <https://doi.org/10.1021/acsami.9b21713>
- İlhan, G. T., Irmak, G., & Gümüşderelioğlu, M. (2020). Microwave assisted methacrylation of Kappa carrageenan: A bioink for cartilage tissue engineering. *International Journal of Biological Macromolecules*, 164, 3523–3534. <https://doi.org/10.1016/j.ijbiomac.2020.08.241>
- Jalil, A., Khan, S., Naeem, F., Haider, M. S., Sarwar, S., Riaz, A., & Ranjha, N. M. (2017). The structural, morphological and thermal properties of grafted pH-sensitive interpenetrating highly porous polymeric composites of sodium alginate/acrylic acid copolymers for controlled delivery of diclofenac potassium. *Designed Monomers and Polymers*, 20(1), 308–324.  
<https://doi.org/10.1080/15685551.2016.1259834>

- Jeon, O., Song, S. J., Lee, K.-J., Park, M. H., Lee, S.-H., Hahn, S. K., Kim, S., & Kim, B.-S. (2007). Mechanical properties and degradation behaviors of hyaluronic acid hydrogels cross-linked at various cross-linking densities. *Carbohydrate Polymers*, *70*(3), 251–257. <https://doi.org/10.1016/j.carbpol.2007.04.002>
- Jia, W., Fang, F., Ma, X., & Wang, L. (2023). Electrochemical and mechanical properties for silver nanoparticles-sodium alginate bio-composites electroactive actuator. *Cellulose*, *30*(10), 6317–6331. <https://doi.org/10.1007/s10570-023-05257-x>
- Kim, E., Kim, M. H., Song, J. H., Kang, C., & Park, W. H. (2020). Dual crosslinked alginate hydrogels by riboflavin as photoinitiator. *International Journal of Biological Macromolecules*, *154*, 989–998. <https://doi.org/10.1016/j.ijbiomac.2020.03.134>
- Kopeček, J., & Yang, J. (2007). Hydrogels as smart biomaterials. *Polymer International*, *56*(9), 1078–1098. <https://doi.org/10.1002/pi.2253>
- Kuo, C. K., & Ma, P. X. (2008). Maintaining dimensions and mechanical properties of ionically crosslinked alginate hydrogel scaffolds in vitro. *Journal of Biomedical Materials Research Part A*, *84A*(4), 899–907. <https://doi.org/10.1002/jbm.a.31375>
- Lee, K. Y., & Mooney, D. J. (2012). Alginate: Properties and biomedical applications. *Progress in Polymer Science*, *37*(1), 106–126. <https://doi.org/10.1016/j.progpolymsci.2011.06.003>
- Li, S., Xiong, Q., Lai, X., Li, X., Wan, M., Zhang, J., Yan, Y., Cao, M., Lu, L., Guan, J., Zhang, D., & Lin, Y. (2016). Molecular Modification of Polysaccharides and Resulting Bioactivities: Molecular modification of polysaccharides.... *Comprehensive Reviews in Food Science and Food Safety*, *15*(2), 237–250. <https://doi.org/10.1111/1541-4337.12161>
- Luo, M., Zhang, X., Wu, J., & Zhao, J. (2021). Modifications of polysaccharide-based biomaterials under structure-property relationship for biomedical applications. *Carbohydrate Polymers*, *266*, 118097. <https://doi.org/10.1016/j.carbpol.2021.118097>

- Lv, Y., Ma, X., Xu, Y., Shu, H., & Jia, W. (2022). Effect of carboxymethyl cellulose on the output force and electrochemical performance of sodium alginate ion electric actuator. *Sensors and Actuators A: Physical*, 339, 113269. <https://doi.org/10.1016/j.sna.2021.113269>
- Mahou, R., Borcard, F., Crivelli, V., Montanari, E., Passemard, S., Noverraz, F., Gerber-Lemaire, S., Bühler, L., & Wandrey, C. (2015). Tuning the Properties of Hydrogel Microspheres by Adding Chemical Cross-linking Functionality to Sodium Alginate. *Chemistry of Materials*, 27(12), 4380–4389. <https://doi.org/10.1021/acs.chemmater.5b01098>
- Mihaila, S. M., Gaharwar, A. K., Reis, R. L., Marques, A. P., Gomes, M. E., & Khademhosseini, A. (2013). Photocrosslinkable *Kappa* -Carrageenan Hydrogels for Tissue Engineering Applications. *Advanced Healthcare Materials*, 2(6), 895–907. <https://doi.org/10.1002/adhm.201200317>
- Ouwerx, C., Velings, N., Mestdagh, M. M., & Axelos, M. A. V. (1998). Physico-chemical properties and rheology of alginate gel beads formed with various divalent cations. *Polymer Gels and Networks*, 6(5), 393–408. [https://doi.org/10.1016/S0966-7822\(98\)00035-5](https://doi.org/10.1016/S0966-7822(98)00035-5)
- Paepe, I. D., Declercq, H., Cornelissen, M., & Schacht, E. (2002). Novel hydrogels based on methacrylate-modified agarose. *Polymer International*, 51(10), 867–870. <https://doi.org/10.1002/pi.945>
- Roy, P. K., Swami, V., Kumar, D., & Rajagopal, C. (2011). Removal of toxic metals using superabsorbent polyelectrolytic hydrogels. *Journal of Applied Polymer Science*, 122(4), 2415–2423. <https://doi.org/10.1002/app.34384>
- Sahraro, M., Barikani, M., & Daemi, H. (2018). Mechanical reinforcement of gellan gum polyelectrolyte hydrogels by cationic polyurethane soft nanoparticles. *Carbohydrate Polymers*, 187, 102–109. <https://doi.org/10.1016/j.carbpol.2018.01.028>
- Scheja, S., Domanskyi, S., Gamella, M., Wormwood, K. L., Darie, C. C., Poghossian, A., Schöning, M. J., Melman, A., Privman, V., & Katz, E. (2017). Glucose-Triggered Insulin Release from Fe<sup>3+</sup>

- Cross-linked Alginate Hydrogel: Experimental Study and Theoretical Modeling.  
*ChemPhysChem*, 18(12), 1541–1551. <https://doi.org/10.1002/cphc.201700195>
- Schweiger, R. G. (1962). Acetylation of Alginic Acid. I. Preparation and Viscosities of Algin Acetates.  
*The Journal of Organic Chemistry*, 27(5), 1786–1789. <https://doi.org/10.1021/jo01052a072>
- Shang, J., & Theato, P. (2018). Smart composite hydrogel with pH-, ionic strength- and temperature-induced actuation. *Soft Matter*, 14(41), 8401–8407. <https://doi.org/10.1039/C8SM01728J>
- Shi, Q., Liu, H., Tang, D., Li, Y., Li, X., & Xu, F. (2019). Bioactuators based on stimulus-responsive hydrogels and their emerging biomedical applications. *NPG Asia Materials*, 11(1), 64.  
<https://doi.org/10.1038/s41427-019-0165-3>
- Timoshenko, S. (1925). Analysis of Bi-Metal Thermostats. *Journal of the Optical Society of America*, 11(3), 233. <https://doi.org/10.1364/JOSA.11.000233>
- VIEW - 2021—Li—Stimuli-responsive hydrogels Fabrication and biomedical applications-1.pdf. (n.d.).
- Wang, L., Jian, Y., Le, X., Lu, W., Ma, C., Zhang, J., Huang, Y., Huang, C.-F., & Chen, T. (2018). Actuating and memorizing bilayer hydrogels for a self-deformed shape memory function. *Chemical Communications*, 54(10), 1229–1232. <https://doi.org/10.1039/C7CC09456F>
- Wang, X., Huang, H., Liu, H., Rehfeldt, F., Wang, X., & Zhang, K. (2019). Multi-Responsive Bilayer Hydrogel Actuators with Programmable and Precisely Tunable Motions. *Macromolecular Chemistry and Physics*, 220(6), 1800562. <https://doi.org/10.1002/macp.201800562>
- Wei, Z., He, J., Liang, T., Oh, H., Athas, J., Tong, Z., Wang, C., & Nie, Z. (2013). Autonomous self-healing of poly(acrylic acid) hydrogels induced by the migration of ferric ions. *Polymer Chemistry*, 4(17), 4601. <https://doi.org/10.1039/c3py00692a>
- Zanon, M., Chiappone, A., Garino, N., Canta, M., Frascella, F., Hakkarainen, M., Pirri, C. F., & Sangermano, M. (2022). Microwave-assisted methacrylation of chitosan for 3D printable hydrogels in tissue engineering. *Materials Advances*, 3(1), 514–525.  
<https://doi.org/10.1039/D1MA00765C>

Zhao, J., Zhao, X., Guo, B., & Ma, P. X. (2014). Multifunctional Interpenetrating Polymer Network Hydrogels Based on Methacrylated Alginate for the Delivery of Small Molecule Drugs and Sustained Release of Protein. *Biomacromolecules*, *15*(9), 3246–3252.  
<https://doi.org/10.1021/bm5006257>